Biomaterials Science

Accepted Manuscript

This article can be cited before page numbers have been issued, to do this please use: R. Yu, L. Xing, P. Cui, J. Qiao, Y. He, X. Chang, T. Zhou, Q. Jin, H. Jiang and Y. Xiao, *Biomater. Sci.*, 2018, DOI: 10.1039/C8BM00381E.

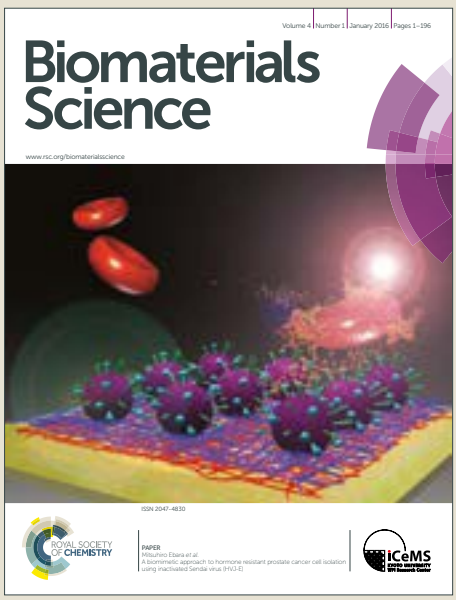

ROYAL SOCIETY OF CHEMISTRY

rsc.li/biomaterials-science

View Article Online
DOI: 10.1039/C8BM00381E

Regulating Golgi Apparatus by co-delivery of COX-2 Inhibitor and Brefeldin A for Suppression of Tumor Metastasis

Ru-Yi Yu[a,1], Lei Xing[a,b,c,d,1], Peng-Fei Cui[a], Jian-Bin Qiao[a], Yu-Jing He[a], Xin Chang[a], Tian-Jiao Zhou[a], Qing-Ri Jin[e,*], Hu-Lin Jiang[a,b,c,d,*], Yanyu Xiao[a,*]

[a] State Key Laboratory of Natural Medicines, Department of Pharmaceutics, China Pharmaceutical University, Nanjing 210009, China

[b] Jiangsu Key Laboratory of Druggability of Biopharmaceuticals, China Pharmaceutical University, Nanjing, 210009, China

[c] Jiangsu Key Laboratory of Drug Screening, China Pharmaceutical University, Nanjing, China

[d] Jiangsu Key Laboratory of Drug Discovery for Metabolic Diseases, China Pharmaceutical University, Nanjing 210009, China

[e] College of Animal Science and Technology, Zhejiang A&F University, Lin'an, Zhejiang 311300, China

* To whom correspondence should be addressed.

Yanyu Xiao, State Key Laboratory of Natural Medicines, Department of Pharmaceutics, China Pharmaceutical University, Nanjing 210009, China

Tel: 025-83271079; E-mail: cpuyanyuxiao@163.com

Hu-Lin Jiang, State Key Laboratory of Natural Medicines, Department of Pharmaceutics, China Pharmaceutical University, Nanjing 210009, P. R. China

View Article Online
DOI: 10.1039/C8BM00381E

Tel: +86-025-83271027; Fax: +86-025-83271027; E-mail: jianghulin3@163.com

Qing-Ri Jin, College of Animal Science and Technology, Zhejiang A&F University, Lin'an, Zhejiang 311300, China

Tel: 0571-63741575; Fax: 0571-63741392; E-mail: qingrijin@163.com

View Article Online
DOI: 10.1039/C8BM00381E

Abstract

The cure of breast cancer is still a medical difficulty in recent years due to main treatment's failure in inhibiting invasion and metastasis of cancer cells, which leads to the recurrence of breast cancer eventually. Many secreted proteins are overexpressed and play a crucial role during tumorigenesis and development. The Golgi apparatus is a key protein processing and secretion factory by which metastasis-associated proteins are modified, transported and secreted, which makes it a viable strategy to inhibit tumor metastasis by regulating Golgi apparatus of tumor cells. Here, celecoxib (CLX) and brefeldin A (BFA) were encapsulated into the biocompatible polymer PLGA-PEG to form nanoparticles acting on Golgi apparatus for treating metastatic breast cancer, they are specific COX-2 inhibitor accumulating in Golgi apparatus and protein transport inhibitor fusing Golgi apparatus into endoplasmic reticulum, respectively. The optimized CLX and BFA co-loaded nanoparticles (CBNPs) possessed good physicochemical properties. CBNPs efficiently damaged Golgi apparatus within 30 min and showed enhanced cytotoxicity of CLX and BFA on the murine metastatic breast cancer 4T1 cells. The cell migration and invasion abilities were dramatically suppressed by CBNPs. Further, the expression and secretion of metastasis-associated proteins such as matrix metalloproteinase-9 (MMP-9) and vascular endothelial growth factor (VEGF) were reduced remarkably. Our findings showed that co-delivering CLX and BFA to regulate Golgi apparatus might be an efficient strategy to inhibit breast cancer growth and suppress tumor cells metastasis.

Keywords: Golgi apparatus, COX-2, Celacoxib, Brefeldin A, Breast cancer,

View Article Online
DOI: 10.1039/C8BM00381E

Metastasis

1. Introduction

Breast cancer is one of the most commonly reported cancers among female in 2016.[1] Researches have shown that 90% of cancer deaths are caused by metastasis, while 30% of breast cancer patients are prone to recurrence within three years after receiving treatment.[2, 3] Currently the clinical treatments of cancer metastasis are limited very much, which merely reducing the pain and prolonging the short-term survival of patients. Tumor metastasis is an invasion-metastasis cascade in which tumor cells overexpress various metastasis-associated proteins, including secreted proteins such as MMP-9 capable of degrading the extracellular matrix, and VEGF involved in tumor angiogenesis.[4, 5]

The Golgi apparatus is an intracellular protein processing and secretion plant by which all the above secreted proteins involved in tumor occurrence and development are modified, transported and secreted.[6, 7] Furthermore, multiple signal pathways in Golgi apparatus are contributed to promoting cell migration.[8] Tumor cells' metabolism and protein secretion activities are particularly exuberant due to the faster proliferation rate than normal cells, so these malignant cells are in the state of hyperplasia which leads Golgi apparatus to become larger.[9] Therefore, the Golgi apparatus of tumor cells can be used as a special target for cancer therapy, and damage to the function and structure of Golgi apparatus is a promising idea for inhibiting tumor cell metastasis.[10]

View Article Online
DOI: 10.1039/C8BM00381E

In relation to the development of Golgi apparatus and tumorigenesis, the most commonly studied cyclooxygenase subtype is COX-2, which is an inducing enzyme accumulating in the Golgi apparatus and the expression of it is increased by a variety of stimuli, such as tissue damage, inflammation or malignant transformation.[11, 12] Celecoxib (CLX) is a specific inhibitor of COX-2, which block the catalytic effect of COX-2 on the promotion of endothelial cell migration, enhanced vascular permeability, and up-regulation of MMP-9 or VEGF expression.[13] Furthermore, it is reported that CLX can inhibit the expression of protein Bcl-2 to interfere with the proliferation of tumor cells, thereby changing the mitochondrial permeability to promote cell apoptosis.[14, 15] Meanwhile, brefeldin A (BFA) is a signal transduction inhibitor acting on Golgi apparatus which will collapse soon and fuse onto the endoplasmic reticulum after incubation.[16, 17] Then intracellular vesicles transport, and secretion pathways of secreted proteins will be restricted. In addition, BFA also elevates the level of endoplasmic reticulum stress in cancer cells by which cell apoptosis mediated by caspase-12 pathway is induced.[18] In the field of drug delivery, the novel combination of CLX and naringin in PLGA nanoparticles can enhance the anticancer effect of the latter in the treatment of lung cancer, and BFA loaded electrospun PEG–PLLA nanofibers have obvious inhibition effect against human liver carcinoma HepG2 cells.[19, 20]

In this work, CLX and BFA were first co-encapsulated into the biocompatible amphiphilic polymer PLGA-PEG to form nanoparticles (CBNPs) for the treatment of tumor metastasis (Scheme 1). The particle size, zeta potential, drug loading,

View Article Online
DOI: 10.1039/C8BM00381E

encapsulation efficiency and release profile of the optimized CBNPs were characterized. The damage degree of Golgi apparatus were evaluated by immunofluorescence staining, western blotting analysis and transmission electron microscope photographs. The anti-tumor effect of CBNPs were evaluated in the metastatic murine breast cancer cells by MTT assay, live/dead cells double stain and apoptosis assay. Further, the inhibiting effect and mechanism on the migration and invasion abilities of 4T1 cells were also studied.

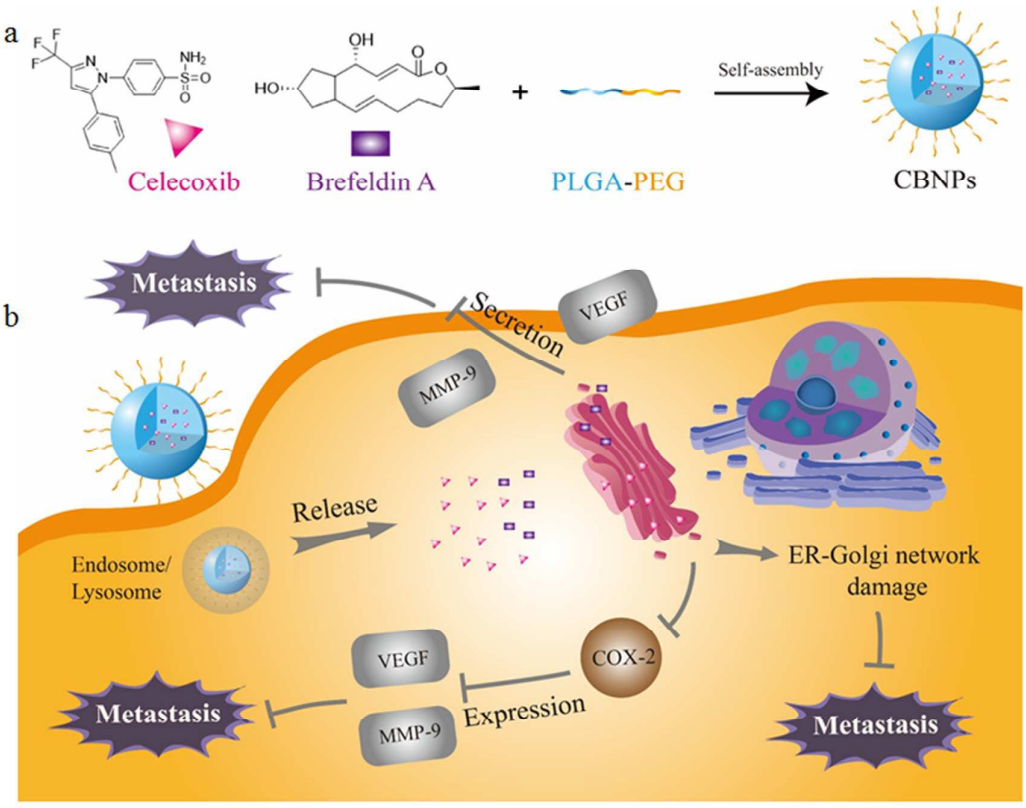

Scheme 1 (a) The biocompatible amphiphilic polymer PLGA-PEG co-assembles with CLX and BFA to form stable nanoparticles (CBNPs). (b) After being endocytosed into tumor cells, CBNPs can achieve effective lysosomal escape, drugs are released and spread to the Golgi apparatus. CLX inhibits the activity of COX-2 in the Golgi

View Article Online
DOI: 10.1039/C8BM00381E

apparatus and down-regulates the expression of MMP-9 and VEGF. On the other hand, the Golgi apparatus cannot modify and secrete the residual MMP-9 and VEGF due to the injury by BFA. CLX and BFA play a role in inhibiting tumor cell metastasis while damaging the tumor cells synergistically.

2. Materials and methods

2.1. Materials

$PLGA_{5k}$-PEG_{2k} with terminal methoxy groups was purchased from Jinan Daigang Biomaterial Co., Ltd (Jinan, China). Celecoxib (CLX) was purchased from J&K Scientific Ltd (Beijing, China). Brefeidin A (BFA) was purchased from Chembest Research Laboratories Ltd (Shanghai, China). Coumarin 6 was procured from TCI (Tokyo, Japan). Crystal violet was obtained from Sinopharm Chemical Reagent Co., Ltd (Nanjing, China). Calcein-AM/PI Double Stain Kit was purchased from Shanghai YEASEN Biotechnology Co., Ltd (Shanghai, China). Hoechst 33342, 3-(4,5-dimethyl-2-thiazolyl)-2,5-diphenyl-2-H-tetrazolium bromide (MTT), Hank's Balanced Salt Solution (HBSS), Annexin V-FITC/PI Apoptosis Detection Kit, Dulbeco's Modified Eagle Medium (DMEM), BCA Protein Assay Kit and Goat Anti-Rabbit IgG were obtained from KeyGEN BioTECH (Nanjing, China). LysoTracker® Red DND-99 and fetal bovine serum (FBS) were procured from Thermo Fisher Scientific (Waltham, MA, USA). Matrigel was procured from Becton, Dickinson and Company (New York, USA). Anti-GM130 antibody, anti-MMP-9 antibody, anti-VEGF antibody and Goat Anti-Rabbit IgG H&L (Alexa Fluor® 488)

View Article Online
DOI: 10.1039/C8BM00381E

were purchased from Abcam (Shanghai, China). All other reagents are of analytical grade and used without further purification.

2.2. Preparation of CLX and BFA co-loaded nanoparticles (CBNPs)

The preparation of CBNPs was based on a modified film dispersion method with some experimental steps referenced elsewhere.[21, 22] Firstly, PLGA-PEG, CLX and BFA were added to a 50 mL round bottom flask and dissolved in 3 mL of acetone. Secondly, the organic solvent was removed by a rotary evaporator at 40 °C to form a transparent film. Next, the remaining organic solvent was eliminated by a vacuum drier at 40 °C for 3 days. Finally, 4 mL of preheated 5% glucose solution was added to the flask, and the nanoparticles were dispersed by sonication at 40 °C for 20 min. The resulting solution was centrifuged at 2500 rpm for 5 min to remove unencapsulated drugs.

2.3. Particle size and zeta potential measurements

The particle size and zeta potential were measured by ZetaPlus particle size and zeta potential analyzer (Brookhaven Instruments, USA) at room temperature. The mean value was recorded as the average of three measurements.

2.4. Observation of transmission electron microscopy

A drop of CBNPs was dripped onto a copper grid, dried at room temperature for 2 min, and the filter paper was used to remove redundant liquid. Then a drop of 1% phosphotungstic acid solution was added and dried at room temperature for 2 min. The excess liquid was removed with filter paper and dried at room temperature. The

View Article Online
DOI: 10.1039/C8BM00381E

micrographs of CBNPs were observed on a transmission electron microscope (JEM-200CX, JEOL, Japan) of 100 kV acceleration voltage.

2.5. Determination of drug content

One hundred μL of CBNPs were dispersed in equal volume of methanol and filtered through a 0.45 μm organic microporous membrane. The response value of drug was measured on a Shimadzu LC-20A (PDA) HPLC (Column: Ultimate XB C18, 4.6 mm × 250 mm, 5 μm) and the mobile phase was set to methanol: water = 85: 15 at a flow rate of 0.8 mL/min. Detection wavelengths of CLX and BFA were 250 and 230 nm, respectively. Then the drug content was calculated based on the standard curve established by HPLC.

2.6. Stability of CBNPs

CBNPs were dispersed in 5% glucose solution, sequentially diluted in different times, and the particle size was measured every day for three days to obtain the dilution stability curve. Meanwhile, CBNPs were dispersed in equal volume of 5% glucose solution, and placed at room temperature or 4 ℃ refrigerator. The particle size was measured every day within one week to obtain the temperature stability curve. The appropriate amount of nanoparticles were dispersed in equal volume of PBS, distilled water, DMEM medium and 10% FBS for one week to get the solvent stability curve. Finally, CBNPs were placed at room temperature for a long period to obtain the storage stability curve.

2.7. Release profiles of CLX and BFA from CBNPs *in vitro*

View Article Online
DOI: 10.1039/C8BM00381E

Five hundred μL of CBNPs were placed in 3500 Da dialysis bag and then placed into a conical flask containing 25 mL of PBS. The sample was set at a constant temperature shaker (120 rpm, 37 ℃). Tow mL of dissolution medium was taken out at 0, 15, 30 min, 1, 2, 4, 6, 8, 10, 12, 24, 36, 48, 72, 96 h and equal volume of PBS was added into the conical flask. All samples were filtered through a 0.45 μm microporous membrane and the drug content was measured by HPLC. Then the drug content was calculated based on the standard curve established by HPLC. Further the cumulative release amount and cumulative release percentage of CLX and BFA were obtained.

2.8. Cell culture

The murine mammary carcinoma cell line 4T1 and human cervical cancer cell line HeLa were purchased from American type culture collection (ATCC), and cultured in DMEM containing 10% FBS. Cells were cultured in a 37 ℃ incubator containing 5% carbon dioxide.

2.9. Cellular uptake of PLGA-PEG nanoparticles

4T1 cells were seeded in 24-well plates and cultured for 24 h. Then, free coumarin 6 or coumarin 6-loaded PLGA-PEG nanoparticles were added and incubated with cells for 2, 4 and 6 h, respectively. Subsequently, cells were washed with HBSS followed by photographed under an inverted fluorescence microscope. Finally, cells were harvested for fluorescence quantification on a flow cytometer.

2.10. Lysosomal escape evaluation of PLGA-PEG nanoparticles

The lysosomal escape ability was evaluated according to our previous reported

View Article Online
DOI: 10.1039/C8BM00381E

method.[23] 4T1 cells were seeded in 35 mm glass-bottomed petri dishes at 1×10^5 cells per dish and cultured for 24 h. Subsequently, cells were incubated with coumarin 6-loaded PLGA-PEG nanoparticles for 30 min, 2 and 4 h, respectively. Afterwards, 100 nM LysoTracker red DND-99 was added and incubated for 1 h. Subsequently, Hoechst 33342 was added for 30 min to dye the nucleus and cells were observed by a confocal laser scanning microscope (CLSM).

2.11. Detection of the damage degree of Golgi apparatus by immunofluorescent staining and transmission electron microscopy

HeLa cells were applied as a model to observe the changes of Golgi apparatus by immunofluorescent staining because of the high expression amount of Golgi matrix protein GM130.[24, 25] Firstly, cells were seeded in 35 mm glass-bottomed petri dishes and cultured for 18 h. Blank PLGA-PEG nanoparticles (PPNPs), free CLX solution, free BFA solution, physical mixing of dual drugs and CBNPs were incubated with cells for 30 min, 1 and 2 h, respectively. Secondly, cells were washed with HBSS for 5 minutes three times (on a decanter shaker) and fixed with 4% paraformaldehyde for 20 min at room temperature. Thirdly, cells were permeabilized with 0.2% Triton X-100 for 3 min at room temperature. Fourthly, cells were blocked with 5% goat serum for 30 min at room temperature. Afterwards, goat serum was removed and anti-GM130 antibody was added into petri dishes, and cells were incubated overnight at 4 °C. Then, corresponding second antibody was added and cells were incubated for 30 min in the dark. Next, Hoechst 33342 was added and incubated for 15 min. Finally, cells were sealed with 50% glycerol and visualized by a confocal laser scanning

View Article Online
DOI: 10.1039/C8BM00381E

microscope.

Further, transmission electron microscopy was used to observe morphology changes of intracellular Golgi apparatus. 4T1 cells were seeded in 6-well plates and cultured for 24 h. Then, cells were incubated with PPNPs or CBNPs for an hour. Cells were harvested, fixed with 2.5% glutaraldehyde and pretreated according to the protocol followed by photographing on TEM.

2.12. Cytotoxicity assay and live/dead cells double stain

In vitro cytotoxicity experiments by MTT assay were performed on 4T1 and HeLa cells. 4T1 and HeLa cells were seeded and incubated for 24 h. Subsequently, cells were incubated with PPNPs, free CLX, free BFA, physical mixing of dual drugs and CBNPs for 24 h, respectively. Next, 20 μL of MTT solution (5 mg/mL) was added and incubated for 4 h in 37 °C incubator. Subsequently, 150 μL of dimethyl sulfoxide (DMSO) was added to dissolve formazan crystals. Finally, the absorbance was detected to measure the cell viability on a microplate reader.

Further, Calcein-AM/PI Double Stain Kit was used to assess the cytotoxicity of 4T1 cells.[26] After incubation for 24 h with various formulations including PPNPs, free CLX, free BFA, physical mixing of dual drugs and CBNPs, cells were stained according to the protocol followed by photographing under an inverted fluorescence microscope.

2.13. Cell apoptosis assay

4T1 cells were seeded in 6-well plates at 3×10^5 cells per dish and incubated in

View Article Online
DOI: 10.1039/C8BM00381E

37 °C incubator for 24 h. Then, PPNPs, free CLX, free BFA, physical mixing of dual drugs and CBNPs were added and incubated with cells for 24 h. Next, 500 μL of EDTA-free trypsin was added to harvest the cells followed by centrifuging at 2000 rpm for 3 min. Afterwards, cells were washed with HBSS and 200 μL of binding buffer was added to resuspend the cells. Five μL of Annexin V-FITC dye and 5 μL of PI dye were sequentially added and reacted at room temperature for 15 min in the dark. Finally, the binding buffer was added to 500 μL and the degree of apoptosis was quantified by a flow cytometer according to our previous study.[27]

2.14. Cell migration and invasion assay

Cell migration activity of 4T1 cells treated with various formulations were assessed by a wound healing test.[28] 4T1 cells were seeded in 6-well plates at 3×10^5 cells per dish and incubated for 36 h. Next, a 10 μL pipette tip was used to scratch the middle of wells and cells were washed twice with HBSS to remove floating cells. Afterwards, PPNPs, free CLX, free BFA, physical mixing of dual drugs and CBNPs were added and incubated with cells for 24 and 48 h, respectively. Cells of each group were photographed to observe the wound healing extent at 0, 24 and 48 h.

Further, a transwell device was used to assess the migration and invasion abilities of 4T1 cells.[29] 4T1 cells were incubated with PPNPs, free CLX, free BFA, physical mixing of dual drugs and CBNPs for 24 h. Subsequently, cells were harvested and resuspended in incomplete DMEM media. For migration assays, 1×10^5 cells in 100 μL of FBS-free media were added to the upper chambers of inserts in a 24-well plate

View Article Online
DOI: 10.1039/C8BM00381E

with pore size of 8.0 μm. For invasion assays, 100 μL of Matrigel matrix was overlaid in upper chambers of inserts and 2×10^5 cells in 100 μL of FBS-free media were added to the upper chambers of inserts. Then 600 μL of DMEM media containing 10% FBS were added into the lower chamber of a 24-well plate. After incubation for 24 h in 37 ℃ incubator, cells across the transwell chambers were stained with crystal violet and photographed under an inverted fluorescence microscope. Finally, 33% acetic acid was used to dissolve the crystal violet for detecting the absorbance at 570 nm on a microplate reader.

2.15. Western blotting analysis

Proteins of intracellular substances and cell culture media were detected by western blotting analysis. After that, 4T1 cells were treated with various formulations (PPNPs, free CLX, free BFA, physical mixing of dual drugs and CBNPs). For secreted proteins, the supernatant was collected, and centrifuged at 2000 rpm for 10 minutes followed by freeze-drying to concentrate proteins. For intracellular proteins, cells were solubilized with lysis buffer for 30 min on ice (vortexed every 5 minutes). Subsequently, cells were centrifuged at 12000 rpm for 5 min to collect the supernatant. Next, the protein concentration was measured by a BCA Protein Assay Kit, meanwhile proteins were boiled for 5 min and separated on a 10% SDS-PAGE. Subsequently, the protein bands were transferred to an NC membrane and blocked with TBST solution containing 5% skim milk powder for 2 h at room temperature. Afterwards, the membrane was incubated overnight at 4 ℃ with primary antibody diluted with TBST solution and then incubated with the corresponding secondary

View Article Online
DOI: 10.1039/C8BM00381E

antibody for 2 h at room temperature. After being washing with TBST three times, bands were visualized with enhanced chemiluminescence (ECL) detection reagents and visualized by a CCD imaging system (Tanon 4200, China).

2.16. Statistical analysis

All results were presented as the means ± standard deviation (SD). Statistical analysis was performed by one-way ANOVA using IBM SPSS statistics 22. ***P<0.001, **P<0.01, *P<0.05. NS, not significant.

3. Results

3.1. Preparation and characterizations of CBNPs

The particle size, polydispersity index (PDI), drug loading and encapsulation efficiency of nanoparticles were compared to obtain the final prescription. When the mass ratio of CLX to BFA was 10: 1 was the best prescription, at the same time, when the mass ratio was greater than 10: 1, the encapsulation rate dropped to 50% approximately (Table 1). The particle size and zeta potential of final CBNPs were 79.2±0.6 nm and -4.3±1.9 mV (Table 2 and Fig. 1a), which were suitable for *in vivo* application according to enhanced permeability and retention effect (EPR).[30-32]

Table 1 Prescription optimization of CBNPs.

CLX / BFA (weight ratio)	Size (nm)	PDI	Drug loading (%)	Encapsulation efficiency (%)
1:1	129.8±2.2	0.162±0.026	2.08±2.33	105.89±1.93
2:1	109.0±4.9	0.228±0.042	1.21±1.47	81.41±1.35

View Article Online
DOI: 10.1039/C8BM00381E

5:1	80.2±0.1	0.187±0.047	0.68±1.52	57.83±1.64
8:1	82.0±1.2	0.178±0.013	0.97±2.12	88.86±2.15
10:1	79.2±0.6	0.204±0.017	2.67±1.41	99.19±2.33
15:1	84.3±2.5	0.216±0.021	1.49±2.01	50.28±1.05

Table 2 Characterizations of CBNPs. The size, zeta potential, drug loading, encapsulation efficiency and drug concentration of PPNPs and CBNPs.

Groups	Size (nm)	Zeta potential (mV)	Drug loading (%)	Encapsulation efficiency (%)	Drug concentration (μg/mL)
PPNPs	69.6±1.7	-13.9±0.8	——	——	——
CBNPs	79.2±0.6	-4.3±1.9	2.7±1.4	99.2±2.3	2936.4[a] / 291.7[b]

Note: a and b indicate concentration of CLX (a) and BFA (b), respectively.

Chromatogram and UV spectra of dual drugs detected by HPLC also showed that dual drugs were successfully encapsulated in nanoparticles (Fig. 1b and Fig. S1). Drug loading and encapsulation efficiency of CBNPs were 2.7±1.4 and 99.2±2.3%, respectively (Table 2). TEM was applied to illustrate the morphology of the final CBNPs. Photomicrographs showed that the nanoparticles were smooth round spheres with a uniform size distribution (Fig. 1c). As shown in Fig. 1d and S2, at pH 7.4, the release extent of BFA and CLX could reach 68.4 and 58.4% at 24 h. After 48 h, the release extent reached up to 96.1 and 80.6%, respectively. The stability experiments showed that CBNPs could maintain a stable particle size distribution at different dilution times, temperatures and solvents in a long time (Fig. 1e-h).

View Article Online
DOI: 10.1039/C8BM00381E

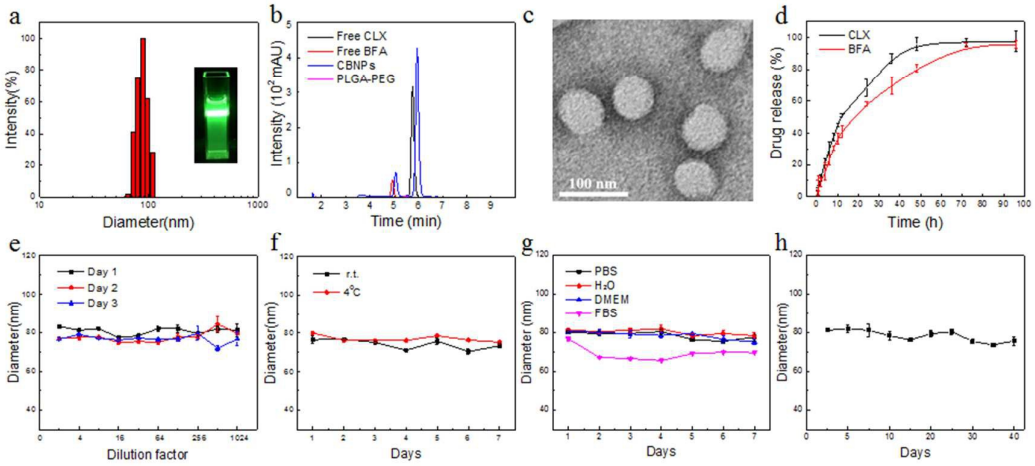

Fig. 1 (a) Histogram of particle-size distribution of CBNPs obtained by dynamic light scattering measurements (Inset photographs: Tyndall effect of CBNPs). (b) Chromatogram of CLX and BFA by HPLC. (c) The transmission electronic microscope image of CBNPs. (d) Drug release profiles of dual drugs in PBS (pH 7.4). (e) Dilution stability of CBNPs within three days. (f) Temperature stability of CBNPs at r.t or 4 °C within one week. (g) Solvent stability of CBNPs mixed with different solvents within one week. (h) Long-term storage stability of CBNPs.

3.2. Cellular uptake of PLGA-PEG nanoparticles

As shown in the Fig. 2a, when cells were incubated with drugs, cells in group coumarin 6-loaded nanoparticles had a stronger fluorescence than group free coumarin 6 and the fluorescence intensity was increased with the passage of time. The same conclusions were obtained with the semi-quantitation results by flow cytometry (Fig. 2b).

View Article Online
DOI: 10.1039/C8BM00381E

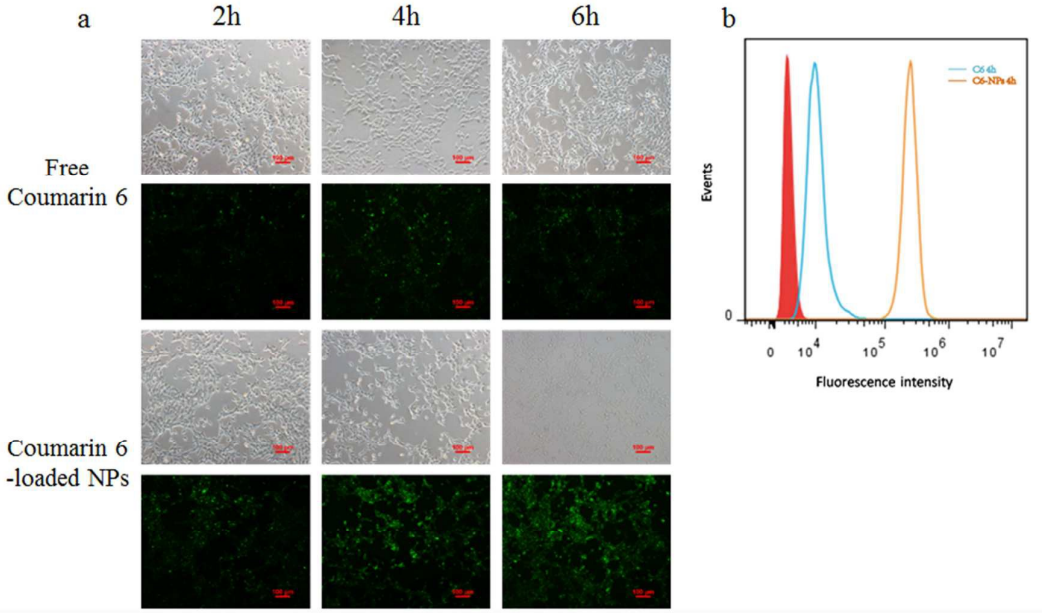

Fig. 2 Cellular uptake of free Coumarin 6 or Coumarin 6-loaded NPs in 4T1 cells after incubation for 2, 4 and 6 h, and (a) photographed by invert fluorescent microscope and (b) quantified by FACS. Scale bars indicate 100 μm.

3.3. Lysosomal escape evaluation of PLGA-PEG nanoparticles

After endocytosis into cells, nanovectors are supposed to escape from the lysosome and diffuse to the cytoplasm to play the pharmacodynamic effect. Studies have shown that PLGA-PEG has the ability of lysosomal escape.[33] Here, CLSM was applied to evaluate the lysosomal escape capacity of PLGA-PEG nanoparticles as shown in the Fig. 3. When cells were incubated with coumarin 6-loaded nanoparticles for 30 min, the green fluorescence of the drug was completely overlapped with the red fluorescence of the lysosome, implying that most of the drug got trapped in lysosomes. After incubation for 2 h, the green fluorescence and the red fluorescence appeared to separate, most of the drug was released from the lysosome. After four hours, the drug

View Article Online
DOI: 10.1039/C8BM00381E

diffused to the entire cytoplasm ultimately.

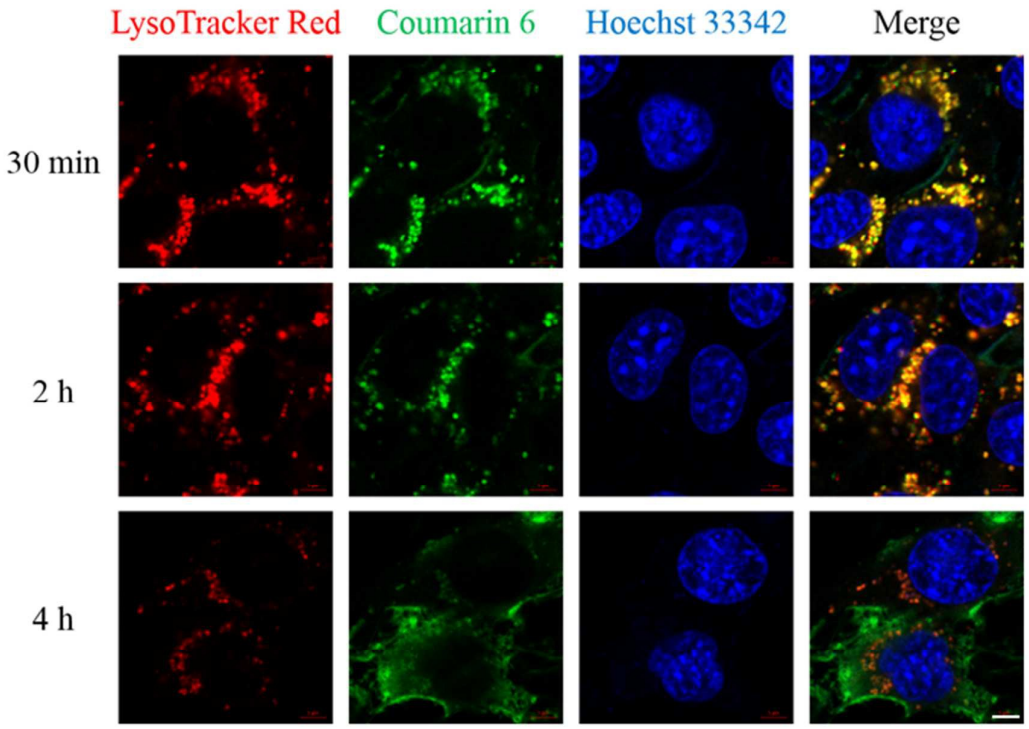

Fig. 3 CLSM images of lysosomal escape evaluation of PLGA-PEG NPs in 4T1 cells after incubation for 30 min, 2 and 4 h. Lysosomes were labelled with LysoTracker red and cell nuclei were stained with Hoechst 33342 (blue). Green fluorescence was represented for coumarin 6. Scale bars indicate 5 μm.

3.4. Detection of the damage degree of Golgi apparatus

BFA is a fungal macrolide antibiotic specifically acting on the organelle Golgi apparatus for inhibiting proteins transport. After incubated with BFA, the Golgi apparatus will collapse within 30 min and fuse onto endoplasmic reticulum, which in turn affects the protein secretion pathways of cells.[34-36] As shown in Fig. 4a, CLSM was used to monitor the shape and structure of Golgi apparatus. After incubation for 30 min, the Golgi apparatus of cells in group control, CLX, BFA and physical mixing

View Article Online
DOI: 10.1039/C8BM00381E

of dual drugs were intact strips. However, Golgi apparatus of cells in group CBNPs appeared to become slight spots, which represented the slight damage of the Golgi apparatus. After incubation for 1 h, the Golgi apparatus in group BFA, the physical mixing of dual drugs and CBNPs showed different degrees of damage. After incubation for another one hour, Golgi apparatus of cells in CBNPs was complete punctate and decreased in quantity, which meant protein GM130 scattered in the cytoplasm was gradually degraded by cells. It was noteworthy that CLX had no damaging effects on Golgi apparatus within a short time, the Golgi apparatus showed no change after incubated with CLX for 2 h.

According to the western blotting experiments, the effect of CLX on the intracellular Golgi apparatus was negligible which had a similar protein band as the control group after incubation for 2 h. BFA and physical mixing of dual drugs did damage to the organelle, but CBNPs' effect to destroy the Golgi apparatus was the best (Fig. 4b), which was consistent with the results of immunofluorescence staining described above.

View Article Online
DOI: 10.1039/C8BM00381E

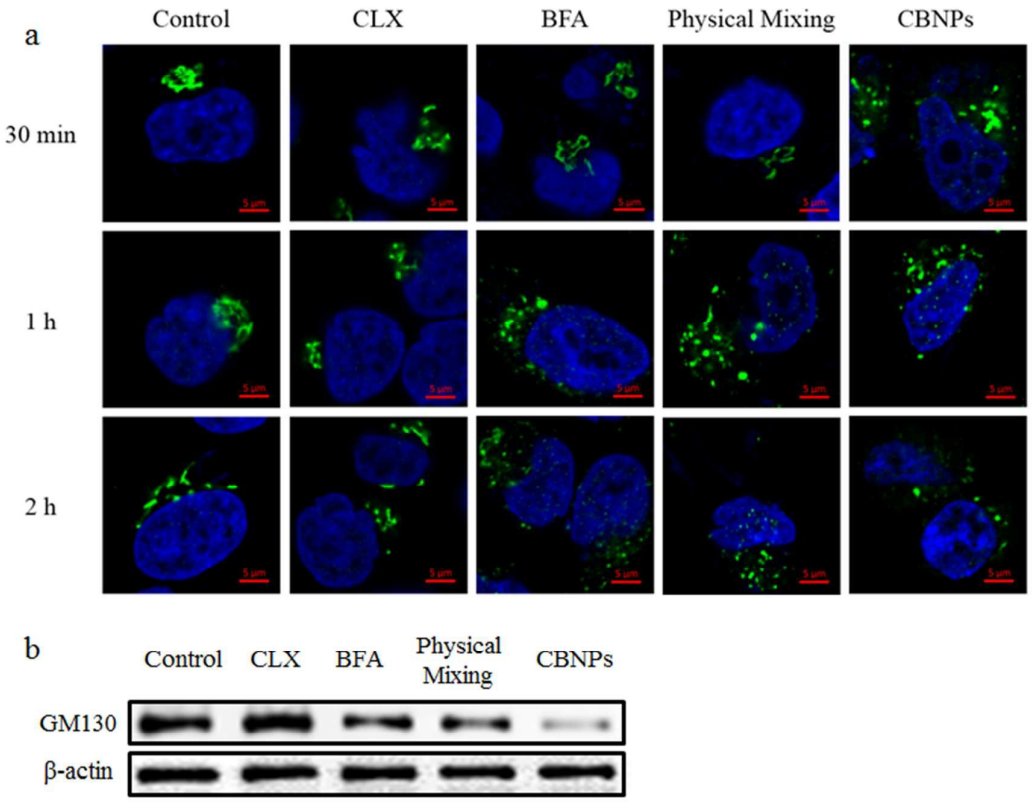

Fig. 4 Detection of the damage degree of Golgi apparatus. (a) CLSM images of the shape of Golgi apparatus after incubation for 30 min, 1 and 2 h, respectively. Golgi apparatus were stained by immunofluorescence staining (green) and cell nuclei were stained with Hoechst 33342 (blue). Scale bars indicate 5 μm. (b) Immunoblotting of GM130 after incubation for 2 h.

Next, cells were fixed with 2.5% glutaraldehyde after incubation with different formulations and the internal morphology was observed by transmission electron microscope. As shown, 4T1 cells in control group presented intact cellular morphology, meanwhile the Golgi apparatus was flat cystic around with a few secreted vesicles (Fig. 5a, b). As for the cells incubated with CBNPs, the cellular morphology remained unchanged and intact, but significant dissociation of the Golgi

View Article Online
DOI: 10.1039/C8BM00381E

apparatus had occurred and no complete flat cystic structure was found in the field of vision (Fig. 5c, d).

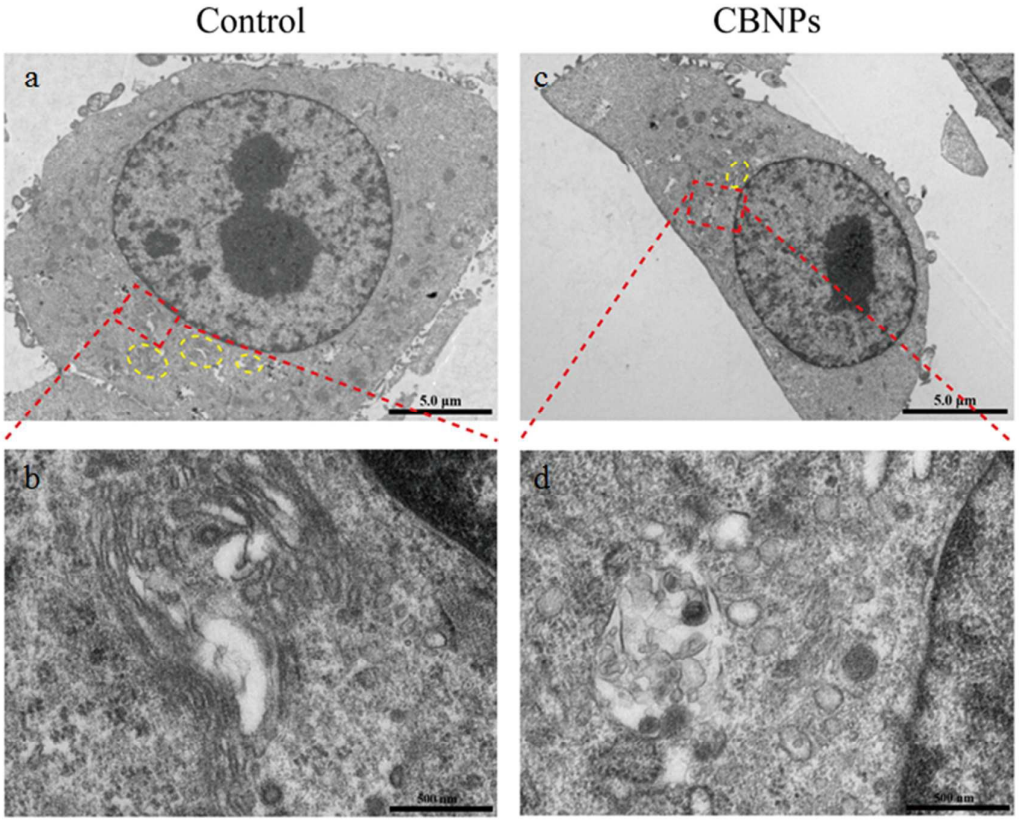

Fig. 5 TEM photographs of (a, c) a whole 4T1 cell (Scale bars indicate 5 μm), and (b, d) intracellular Golgi apparatus (Scale bars indicate 500 nm) after incubation with PPNPs or CBNPs for 1 h. The yellow circles in the figures represent other Golgi apparatus.

3.5. *In vitro* cell toxicity assay

It is reported that CLX can inhibit the expression of protein Bcl-2 to interfere with the proliferation of human prostate cancer cells and colon cancer cells, thereby changing the mitochondrial permeability to promote cell apoptosis.[37, 38] Meanwhile,

View Article Online
DOI: 10.1039/C8BM00381E

Golgi apparatus is supposed to be destroyed within 30 minutes due to the rapid onset of BFA. After prolonged action, as Golgi apparatus within tumor cells collapsed into the endoplasmic reticulum, the ERS level is increased which triggering cell apoptosis ultimately.[18] Compared with CLX, BFA and physical mixing of dual drugs, CBNPs showed a stronger cytotoxic effect on 4T1 cells and cytotoxicity was increased gradually with the increase of drug concentration (Fig. 6a). That was worth mentioning that ethanol had to be used to ensure the dissolution of CLX and BFA due to the hydrophobic nature, therefore greater toxicity was showed at higher concentrations in group physical mixing of dual drugs. Similarly, MTT assays of different drug groups and PLGA-PEG on HeLa cells were also performed (Fig. 6b, c). The results demonstrated that the material PLGA-PEG was non-toxic to cells even at high concentration.

Next, CLX concentration of 15 μg/mL and BFA concentration of 1.5 μg/mL were applied as the concentration for live/dead cells double stain assay and cell apoptosis assay. CLX, BFA and physical mixing of dual drugs showed cytotoxicity on 4T1 cells to some extent, whereas the highest number of dead cells in group CBNPs represented the highest toxicity, which was in accordance with MTT assay (Fig. 6d). Furthermore, CBNPs had an enhanced effect of inducing cell apoptosis compared with CLX, BFA and physical mixing of dual drugs (Fig. 6e).

View Article Online
DOI: 10.1039/C8BM00381E

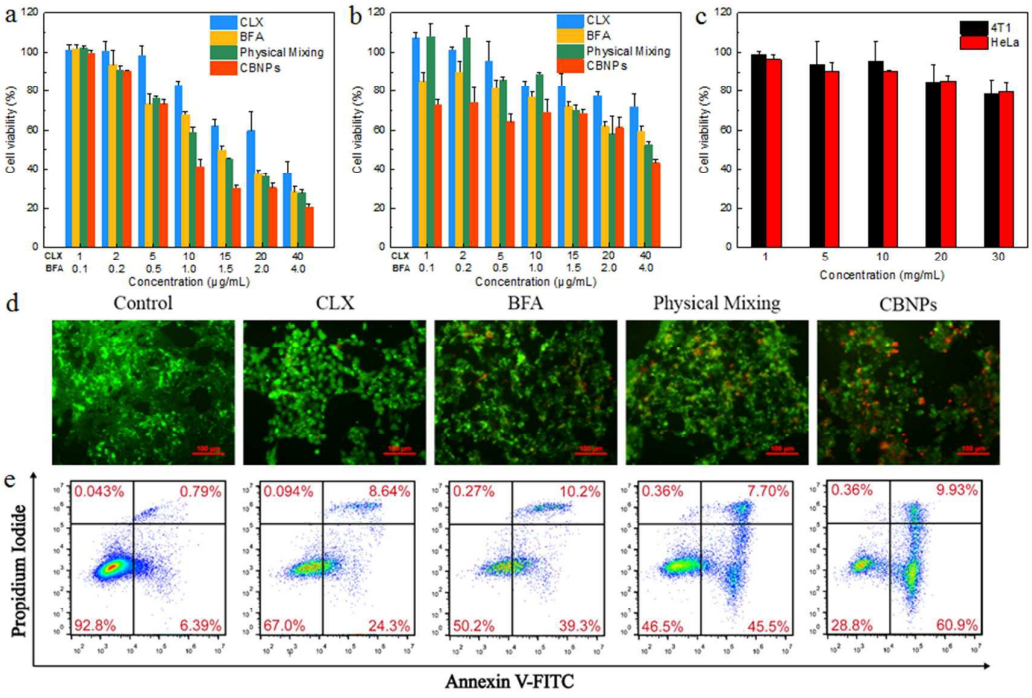

Fig. 6 Evaluation of anti-tumor ability *in vitro*. (a, b) Viability of 4T1 and HeLa cells after incubation for 24 h with free CLX, free BFA, physical mixing of dual drugs and CBNPs at different concentrations. (c) Viability of 4T1 and HeLa cells after incubation for 24 h with PPNPs. (d) Live/dead cell assay for 4T1 cells treated with free CLX, free BFA, physical mixing of dual drugs and CBNPs for 24 h. Scale bars indicate 100 μm. (e) Flow cytometry analysis of cell apoptosis induced by free CLX, free BFA, physical mixing of dual drugs and CBNPs.

3.6. Effect of drugs on cell migration and invasion

Furthermore, abilities for inhibiting cell migration of dual drugs were evaluated. In the wound healing experiment (Fig. 7a), both CLX and BFA inhibited cell migration to some extent as compared with control group. At group physical mixing of dual drugs, the wound healing capacity of cells was inhibited to 80%

View Article Online
DOI: 10.1039/C8BM00381E

approximately which meant both drugs had a common effect in inhibiting cell migration. Further, group CBNPs possessed the strongest inhibition of cell migration and the wound healing rate was as low as 2.1±0.3% (Fig. 7b). The cell migration and invasion assays had consistent results (Fig. 8). Nearly all the cells crossed the transwell membranes at the control group (Fig. 8a). The migration rate and invasion rate of CBNPs were 34.9 and 28.7% which were lower than those of control group and physical mixing of dual drugs (Fig. 8b, c).

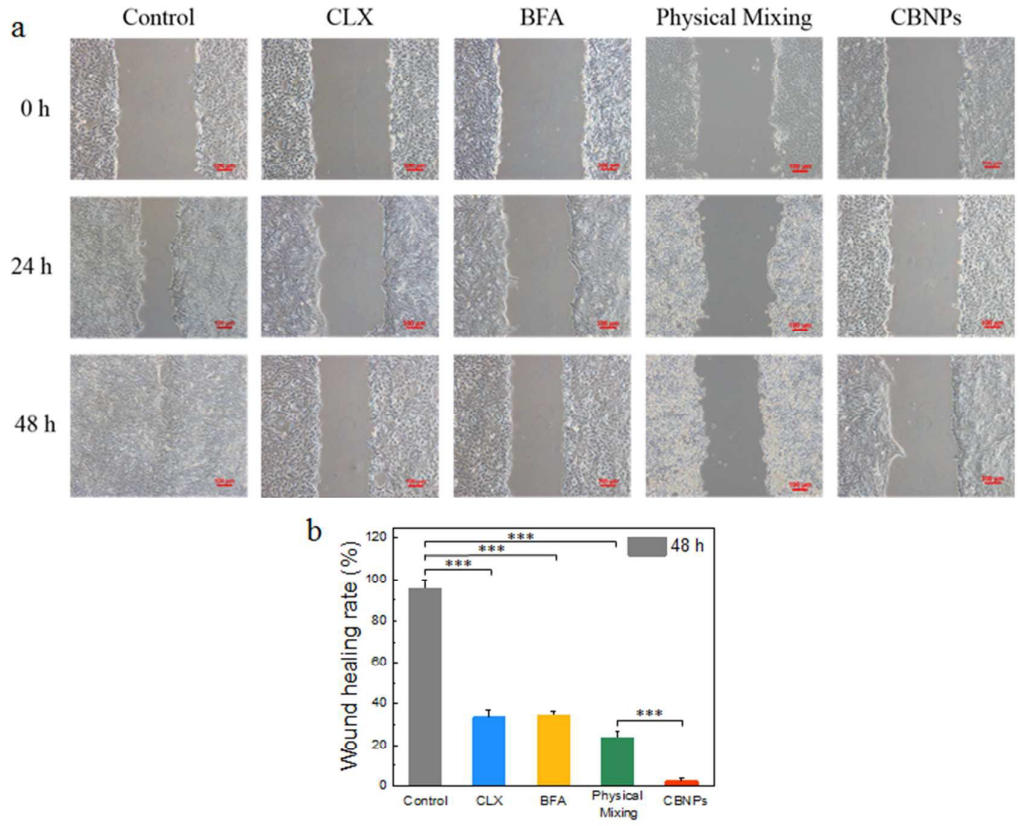

Fig. 7 Wound healing assay. Wound healing ability of 4T1 cells after incubation with free CLX, free BFA, physical mixing of dual drugs and CBNPs for 24, 48 h and (a) photographed by an invert fluorescent microscope and (b) semi-quantified by FlowJo 7.6. Data were given as mean ± SD (n=3). ***P<0.001, **P<0.01, *P<0.05. Scale

View Article Online
DOI: 10.1039/C8BM00381E

bars indicate 100 μm.

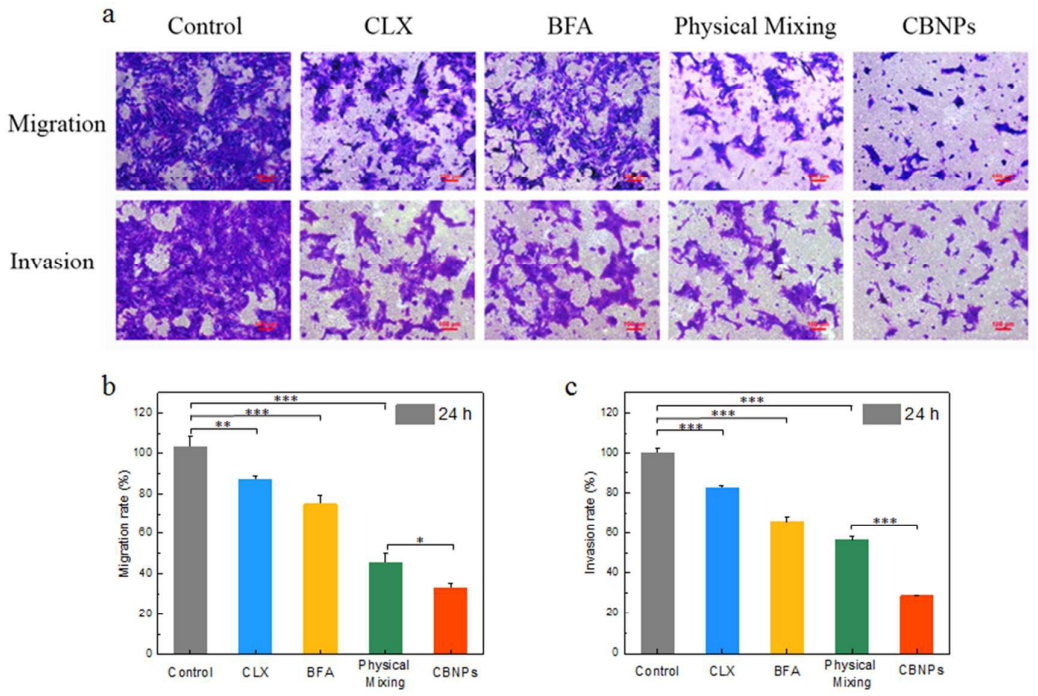

Fig. 8 Cell migration and invasion assays. (a) Invert fluorescent microscope images of 4T1 cells crossing the transwell membrane after incubation with free CLX, free BFA, physical mixing of dual drugs and CBNPs for 24 h, and (b, c) quantified by a microplate reader. Data were given as mean ± SD (n=3). ***P<0.001, **P<0.01, *P<0.05. Scale bars indicate 100 μm.

3.7. Detection of protein expression

It has been shown that COX-2 is overexpressed in various malignancies including breast cancer. Prostaglandins catalytically produced by COX-2 can induce angiogenesis and maintain tumor cell viability and tumor growth.[13] CLX is a specific inhibitor of COX-2, which can down-regulate the expression of metastasis-associated proteins such as MMP-9 and VEGF.[8] Meanwhile, BFA is a protein transport inhibitor

View Article Online
DOI: 10.1039/C8BM00381E

acting on the Golgi apparatus whose morphology will be destroyed.[17] Then the intracellular modification and transport of secreted proteins pathways will be restricted which makes the secretion amount of secreted proteins to be reduced greatly. In this work, CLX and BFA encapsulated in PLGA-PEG could interfere with the expression and secretion of metastasis-associated proteins simultaneously. As shown in Fig. 9, CLX could effectively inhibit the expression of MMP-9 and VEGF after incubation for 24 h, while BFA was more likely to inhibit the secretion of MMP-9 and VEGF to the extracellular matrix. Both drugs could inhibit the biological function of MMP-9 and VEGF synergistically. It was noteworthy that group CBNPs possessed a lower amount of MMP-9 and VEGF in both intracellular and culture media than group physical mixing of dual drugs.

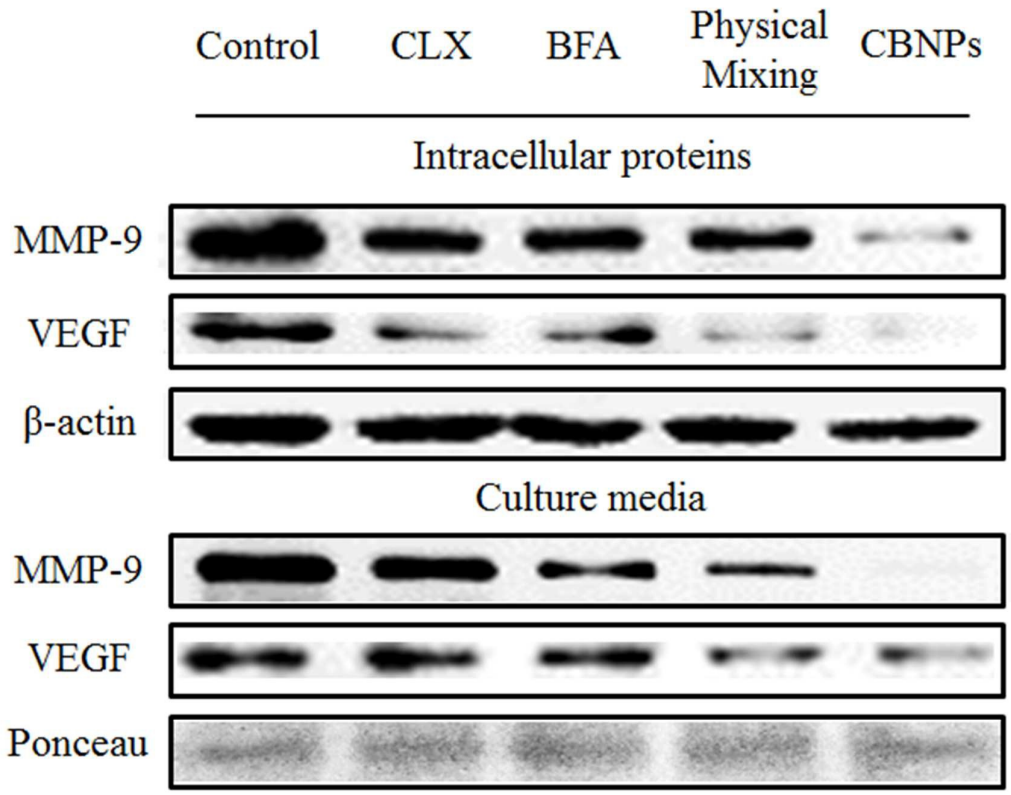

View Article Online
DOI: 10.1039/C8BM00381E

Fig. 9 Representative MMP-9/VEGF protein expression determined by western blotting analysis in 4T1 cells treated with different formulations for 24 h.

4. Discussion

The recurrence and metastasis of cancer is the main cause of death in cancer patients. It is significant for the treatment and prevention of tumor metastasis while treating the primary tumor.[2] The division and cooperation of the organelles are basises for cells to maintain homeostasis.[39] Golgi apparatus is a factory for intracellular protein processing, transportation, and secretion, and is essential for secreted proteins.[40] The Golgi apparatus of tumor cells, like other organelles, is active than normal. Metastasis-associated proteins such as MMP-9 or VEGF are modified and secreted by Golgi apparatus that play a crucial role in tumor metastasis. Thus, regulating Golgi apparatus is a potential method in the treatment of tumor metastasis.

In this experiment, we first formulated CBNPs using PLGA-PEG to encapsulate CLX and BFA for investigating its ability to inhibit the invasion and metastasis of murine breast cancer 4T1 cells (Scheme 1), which are specific inhibitor of COX-2 in Golgi apparatus and protein transport inhibitor, respectively. Optimized CBNPs were formulated by a modified film dispersion method at 40 °C. This might be due to the fact that the glass transition temperature of PLGA-PEG was 33 °C. And when the temperature was higher than this, the mobility of PLGA-PEG segments could be increased, thus effectively encapsulating the drug.[41] CBNPs possessed high drug encapsulation efficiency, sustained cargos release and good stabilities (Table 2, Fig.

View Article Online
DOI: 10.1039/C8BM00381E

1d-h and Fig. S2). TEM photographs showed that CBNPs were well-dispersed, spherical nanoparticles with a diameter of 79.2±0.6 nm (Fig. 1c). The proper particle size allowed CBNPs penetrating the expanding blood vessels of the tumor tissue. Moreover, PLGA-PEG had a good biocompatibility and the zeta potential of CBNPs was slight negative (-4.3±1.9 mV) (Table 2), which would contribute to prevent adsorption between CBNPs and negative charged circulating proteins and prolong the half-life when applied *in vivo*.[42] In addition, CBNPs exhibited rapid cellular uptake and good lysosomal escape potential (Fig. 2 and Fig. 3), which facilitated more drugs to be taken into cells and diffuse into the cytoplasm effectively. In general, the above results made CBNPs a promising nanosystem for cancer chemotherapy.

Next, the effect of CBNPs on the Golgi apparatus and its ability to inhibit proliferation and metastasis of breast cancer cell were evaluated. Encouragingly, CBNPs showed stronger damage ability (Fig. 4a and Fig. 5) and accelerated the disintegration of Golgi matrix proteins GM130 than other formulations (Fig. 4b), which was mainly due to the fact that CBNPs increased the rate of cellular uptake of drugs and enhanced the drug release rate (Fig. 2 and Fig. 3). According to the research, the ERS level will be increased to trigger cell apoptosis after incubation with BFA, and CLX can inhibit the expression of protein Bcl-2 thereby changing the mitochondrial permeability to promote cell apoptosis.[18, 38] As expected, CBNPs exhibited enhanced concentration-dependent toxicity to 4T1 cells compared with single drug or physical mixing of dual drugs while the material PLGA-PEG was basically nontoxic to cells (Fig. 6a, c, d). Meanwhile, CBNPs induced cell apoptosis

View Article Online
DOI: 10.1039/C8BM00381E

effectively and the number of cells entering the apoptotic phase in the CBNPs group was 9.8 times greater than that of the control group (Fig. 6e). In addition, CBNPs strongly inhibited the ability of cells to heal wounds, and suppressed the migration and invasion of 4T1 cells (Fig. 7 and Fig. 8). This might be because CBNPs reduced the expression and secretion of MMP-9 which promotes tumor cell metastasis (Fig. 9), and the damage of Golgi apparatus caused by CBNPs cut down the basic migration ability of cells (Fig. 4 and Fig. 5). Excitingly, the expression and secretion of VEGF were also decreased by CBNPs (Fig. 9), which indicated that CBNPs might be able to restrain the occurrence of tumor neovascularization *in vivo*. To sum up, CBNPs could significantly suppress the growth and metastasis of 4T1 cells by regulating Golgi apparatus.

5. Conclusion

Since Golgi apparatus is the factory for the processing and secretion of intracellular proteins, the regulation of it has a great inhibitory effect on the metastasis of tumor cells. In this work, CLX and BFA were encapsulated into the biocompatible polymer PLGA-PEG to form nanoparticles with a uniform particle size and negative zeta potential. In the murine breast cancer 4T1 cells, CBNPs could damage Golgi apparatus in short period of time and enhance the anti-tumor effect of CLX and BFA. The cell migration and invasion abilities were also suppressed by CBNPs, meanwhile, the expression and secretion of metastasis-associated proteins such as MMP-9 and VEGF were down-regulated observably. Although our strategy has not been validated at the animal level, the strategy of regulating Golgi apparatus has been very effective.

View Article Online
DOI: 10.1039/C8BM00381E

In summary, CBNPs encapsulating CLX and BFA is a promising drug delivery system to simultaneously inhibit growth and metastasis of breast cancer cells by regulating Golgi apparatus.

Acknowledgments

We thank the National Natural Science Foundation of China (Grant No. 81773667, 81573369) and the Open Project of Jiangsu Key Laboratory of Druggability of Biopharmaceuticals (Grant No. 1131730003). We also thank public platform of State Key Laboratory of Natural Medicines for assistance with experimental apparatuses (Confocal Microscopy, Flow Cytometer and HPLC). This work was also supported by the Outstanding Youth Fund of Jiangsu Province of China (Grant No. BK20160031). Part of this work was also funded by the "111" Project from the Ministry of Education of China, the State Administration of Foreign Experts Affairs of China (Grant No. B16046) and Fundamental Research Funds for the Central Universities (2632018PT01 and 2632018ZD12)

Abbreviations

EGFR, epidermal growth factor receptor. MMP-9, matrix metalloproteinase-9. VEGF, vascular endothelial growth factor. PLGA-PEG, poly(lactic-co-glycolic acid - poly(ethylene glycol). CLX, celecoxib. BFA, brefeldin A. COX-2, cyclooxygenase 2. CBNPs, CLX and BFA co-loaded nanoparticles. EPR, enhanced permeability and retention. FBS, fetal bovine serum. MTT, 3-(4, 5-dimethylthiazol-2-yl)-2, 5-diphenyltetrazolium bromide. HBSS, Hank's Balanced Salt Solution. DMEM,

View Article Online
DOI: 10.1039/C8BM00381E

Dulbeco's Modified Eagle Medium. CLSM, confocal laser scanning microscope. ERS, endoplasmic reticulum stress. TEM, transmission electron microscopy. ECL, enhanced chemiluminescence. SD, standard deviation.

References

1. R. L. Siegel, K. D. Miller and A. Jemal, *CA Cancer J Clin*, 2017, **67**, 7-30.
2. P. Mehlen and A. Puisieux, *Nat Rev Cancer*, 2006, **6**, 449-458.
3. E. B. Rankin and A. J. Giaccia, *Science*, 2016, **352**, 175-180.
4. S. Valastyan and R. A. Weinberg, *Cell*, 2011, **147**, 275-292.
5. S. Hirakawa, S. Kodama, R. Kunstfeld, K. Kajiya, L. F. Brown and M. Detmar, *J Exp Med*, 2005, **201**, 1089-1099.
6. R. M. Rios and M. Bornens, *Current Opinion in Cell Biology*, 2003, **15**, 60-66.
7. J. G. Donaldson and J. Lippincott-Schwartz, *Cell*, 2000, **101**, 693-696.
8. V. Millarte and H. Farhan, *ScientificWorldJournal*, 2012, **2012**, 498278.
9. F. Xue, Y. Wen, P. Wei, Y. Gao, Z. Zhou, S. Xiao and T. Yi, *Chem Commun (Camb)*, 2017, **53**, 6424-6427.
10. D. Wlodkowic, J. Skommer, D. McGuinness, C. Hillier and Z. Darzynkiewicz, *Leuk Res*, 2009, **33**, 1440-1447.
11. J. L. Masferrer, K. M. Leahy, A. T. Koki, B. S. Zweifel, S. L. Settle, B. M. Woerner, D. A. Edwards, A. G. Flickinger, R. J. Moore and K. Seibert, *Cancer Research*, 2000, **60**, 1306-1311.
12. H. Zhang, J. Fan, J. Wang, S. Zhang, B. Dou and X. Peng, *Journal of the American Chemical Society*, 2013, **135**, 11663-11669.
13. S. Gately and W. W. Li, *Seminars in Oncology*, 2004, **31**, 2-11.
14. J. L. Masferrer, K. M. Leahy, A. T. Koki, B. S. Zweifel, S. L. Settle, B. M. Woerner, D. A. Edwards, A. G. Flickinger, R. J. Moore and K. Seibert, *Cancer Research*, 2000, **60**, 1306-1311.
15. G. Steinbach, P. M. Lynch, R. K. Phillips, M. H. Wallace, E. Hawk, G. B. Gordon, N. Wakabayashi, B. Saunders, Y. Shen and T. Fujimura, *New England Journal of Medicine*, 2000, **342**, 1946-1952.
16. A. Nebenführ, C. Ritzenthaler and D. G. Robinson, *Plant Physiology*, 2002, **130**, 1102-1108.
17. M. Pavelka and J. Roth, *Brefeldin A-Induced Golgi Apparatus Disassembly*, Springer Vienna, 2010.
18. D. T. Rutkowski and R. J. Kaufman, *Trends in Cell Biology*, 2004, **14**, 20-28.
19. R. Said-Elbahr, M. Nasr, M. A. Alhnan, I. Taha and O. Sammour, *European Journal of Pharmaceutics & Biopharmaceutics*, 2016, **103**, 1-12.
20. W. Liu, J. Wei, P. Huo, Y. Lu, Y. Chen and Y. Wei, *Materials Science & Engineering C Materials for Biological Applications*, 2013, **33**, 2513-2518.
21. M. A. Obeid, A. M. Gebril, R. J. Tate, A. B. Mullen and V. A. Ferroa, *Int J*

View Article Online
DOI: 10.1039/C8BM00381E

Pharm, 2017, **521**, 54-60.

22. X. Ai, L. Zhong, H. Niu and Z. He, *Asian Journal of Pharmaceutical Sciences*, 2014, **9**, 244-250.
23. J. L. Zhang, J. H. Gong, L. Xing, P. F. Cui, J. B. Qiao, Y. J. He, M. Zhang, J. Y. Lyu, C. Q. Luo, S. A. Che, T. Jin and H. L. Jiang, *Int J Pharm*, 2016, **513**, 612-627.
24. S. L. Rong, F. G. Peng, Z. Z. Hong, L. Z. Lin, C. M. Li, W. Jian, F. L. Yuan, L. Feng, L. Na and Z. H. Cheng, *Chemical Science*, 2017, **8**, 6829-6835.
25. L. Fourriere, S. Divoux, M. Roceri, F. Perez and G. Boncompain, *Journal of Cell Science*, 2016, **129**, 3238-3250.
26. J. Kim, H. R. Cho, H. Jeon, D. Kim, C. Song, N. Lee, S. H. Choi and T. Hyeon, *J Am Chem Soc*, 2017, **139**, 10992-10995.
27. M. Zhang, L. Xing, H. Ke, Y. J. He, P. F. Cui, Y. Zhu, G. Jiang, J. B. Qiao, N. Lu, H. Chen and H. L. Jiang, *ACS Appl Mater Interfaces*, 2017, **9**, 11337-11344.
28. Y. Kuang and B. Xu, *Angew Chem Int Ed Engl*, 2013, **52**, 6944-6948.
29. X. He, H. Cao, H. Wang, T. Tan, H. Yu, P. Zhang, Q. Yin, Z. Zhang and Y. Li, *Nano Lett*, 2017, **17**, 5546-5554.
30. H. Meng, M. Xue, T. Xia, Z. Ji, D. Y. Tarn, J. I. Zink and A. E. Nel, *ACS Nano*, 2011, **5**, 4131-4144.
31. U. Prabhakar, H. Maeda, R. K. Jain, E. M. Sevick-Muraca, W. Zamboni, O. C. Farokhzad, S. T. Barry, A. Gabizon, P. Grodzinski and D. C. Blakey, *Cancer Res*, 2013, **73**, 2412-2417.
32. A. K. Iyer, G. Khaled, J. Fang and H. Maeda, *Drug Discov Today*, 2006, **11**, 812-818.
33. X. Zhang, Y. Dong, X. Zeng, X. Liang, X. Li, W. Tao, H. Chen, Y. Jiang, L. Mei and S. S. Feng, *Biomaterials*, 2014, **35**, 1932-1943.
34. J. Panyam, W. Z. Zhou, S. Prabha, S. K. Sahoo and V. Labhasetwar, *Faseb Journal*, 2002, **16**, 1217-1226.
35. T. Yoshida, C. Chen, M. Zhang and H. C. Wu, *Experimental Cell Research*, 1991, **192**, 389-395.
36. J. B. Helms and J. E. Rothman, *Nature*, 1992, **360**, 352-354.
37. S. Grösch, I. Tegeder, E. Niederberger, L. Bräutigam and G. Geisslinger, *Faseb Journal Official Publication of the Federation of American Societies for Experimental Biology*, 2001, **15**, 2742-2744.
38. A. L. Hsu, T. T. Ching, D. S. Wang, X. Song, V. M. Rangnekar and C. S. Chen, *Journal of Biological Chemistry*, 2000, **275**, 11397-11403.
39. S. Dmitrieff and P. Sens, *Physical Review E Statistical Nonlinear & Soft Matter Physics*, 2011, **83**, 041923.
40. M. A. De Matteis and A. Luini, *Nature Reviews Molecular Cell Biology*, 2008, **9**, 273-284.
41. D. S. Fryer, R. D. Peters, E. J. Kim, J. E. Tomaszewski, J. J. D. Pablo, P. F. Nealey, C. C. White and W. L. Wu, *Macromolecules*, 2001, **34**, 5627-5634.
42. B. F. Zhang, L. Xing, P. F. Cui, F. Z. Wang, R. L. Xie, J. L. Zhang, M. Zhang,

View Article Online
DOI: 10.1039/C8BM00381E

Y. J. He, J. Y. Lyu and J. B. Qiao, *Biomaterials*, 2015, **61**, 178-189.